# ATLAS NOTE

ATLAS-CONF-2012-035

March 10, 2012


# Constraining R-parity violating Minimal Supergravity with $\tilde{\tau}_1$ LSP in a four lepton final state with missing transverse momentum

The ATLAS Collaboration



**Abstract**

This note describes an interpretation of a search for supersymmetry in final states with at least four isolated leptons (electrons or muons) and missing transverse momentum. The search used 2.06 fb$^{-1}$ of proton-proton collision data collected with the ATLAS experiment, and found no significant excess above expectations from Standard Model processes. Limits are shown for the Minimal Supergravity/Constrained Minimal Supersymmetric Standard Model (mSUGRA/CMSSM) with $m_0 = A_0 = 0$, $\mu > 0$ and one $R$-parity violating parameter $\lambda_{121} = 0.032$ at the grand unification scale $m_{\rm GUT}$. Keeping these parameters fixed, values of $m_{1/2} < 800$ GeV are excluded at 95% CL if $\tan\beta < 40$ and $m_{\tilde{\tau}_1} > 80$ GeV. These are the first limits from the LHC experiments on a model with a $\tilde{\tau}_1$ as the lightest supersymmetric particle.

# 1 Introduction

The ATLAS Collaboration has recently released preliminary results of a search for supersymmetry (SUSY) in events with at least four leptons ("lepton" here means an isolated electron or muon only) and moderate missing transverse momentum in proton-proton collisions at a centre of mass energy of $\sqrt{s} = 7$ TeV [1]. The data used correspond to an integrated luminosity of 2.06 fb$^{-1}$. No significant excess above the Standard Model (SM) prediction was observed in either of the two defined signal regions. This note describes an interpretation of this result in a Minimal Supergravity/Constrained Minimal Supersymmetric Standard Model (mSUGRA/CMSSM) scenario [2] with $R$-parity violation (RPV) [3, 4] and a $\tilde{\tau}_1$ lightest supersymmetric particle (LSP), the first such interpretation from an LHC experiment.

This note begins with a description of $R$-parity violation in supersymmetry in Section 2, before describing the specific model used in Section 3. The analysis of Ref. [1] is briefly recapitulated in Section 4, and systematic uncertainties are considered in Section 5. Finally, results and conclusions are presented in Sections 6 and 7. Additional information about the model and selection efficiencies is supplied in the two Appendices.

# 2 $R$-Parity violating SUSY

Supersymmetry [5] is one of the most popular theoretical extensions of the SM, able to stabilise the mass of the Higgs boson and unify gauge couplings through the introduction of "super-partner" fermions and bosons for each SM boson and fermion, respectively. In the most general formulation of SUSY, the proton becomes unstable due to new baryon-and lepton-number violating terms in the superpotential [6]:

$$W_{\mathrm{RPV}} = \lambda_{ijk} L_i L_j \bar{E}_k + \lambda'_{ijk} L_i Q_j \bar{D}_k + \lambda''_{ijk} \bar{U}_i \bar{D}_j \bar{D}_k + \kappa_i L_i H_2. \quad (1)$$

Here, $\lambda_{ijk}$, $\lambda'_{ijk}$ and $\lambda''_{ijk}$ are new Yukawa couplings and the $\kappa_i$ have dimensions of mass, but vanish at the unification scale. The indices $i$, $j$ and $k$ refer to quark and lepton generations. The lepton and quark SU(2) doublet superfields are denoted by $L_i$ and $Q_i$, respectively, while the corresponding singlet superfields are given by $\bar{E}_i$ and $\bar{D}_i$. $H_2$ denotes the Higgs SU(2) doublet superfield that couples to up-like quarks.

The superpotential terms in Equation (1) are often avoided by introducing a new symmetry, whereby a quantum number called *R-parity* is conserved [7]. This symmetry makes the LSP stable, requiring it to carry neither electric nor colour charge on cosmological grounds and allowing for it to be a dark matter candidate [8]. In a collider experiment, production of SUSY particles decaying to the LSP would produce significant amounts of missing transverse momentum, a characteristic that drives many searches for supersymmetric particle production.

It may be, however, that the proton lifetime is protected by another, less stringent, symmetry that allows some of the terms in Equation (1). In this case, the LSP is not stable, and may thus carry electric or colour charge. The distinctive signature of large missing transverse momentum may therefore be lost. The search strategy for RPV SUSY depends strongly on which RPV terms are present and the LSP lifetime. In particular, lepton flavour violation can give rise to events with high lepton multiplicities; one such possibility is considered in this note.

# 3 The BC1 benchmark scenario

The physics scenario considered in this note is based on the BC1 benchmark point proposed in Ref. [9]. It is an $R$-parity violating scenario within the context of the mSUGRA/CMSSM framework, with a $\tilde{\tau}$ LSP. The mSUGRA/CMSSM model with $R$-parity violation is described by six parameters:

$$m_0,\ m_{1/2},\ A_0,\ \tan\beta,\ \mathrm{sign}(\mu),\ \boldsymbol{\Lambda}. \quad (2)$$

Table 1: Masses and dominant branching ratios (BR) for the four least massive particles for the original BC1 benchmark point. Adapted from [9].

| | Mass [GeV] | Channel | BR | Channel | BR |
|---|---|---|---|---|---|
| $\tilde{\tau}_1^-$ | 148 | $\tau^-\mu^\pm e^\mp \overset{(-)}{\nu}_e$ | 50.1% | $\tau^- e^\pm e^\mp \overset{(-)}{\nu}_\mu$ | 49.9% |
| $\tilde{e}_R^-$ | 161 | $e^-\nu_\mu$ | 50.0% | $\mu^-\nu_e$ | 50.0% |
| $\tilde{\mu}_R^-$ | 161 | $\tilde{\tau}_1^\pm\tau^\mp\mu^-$ | 99.9% | | |
| $\tilde{\chi}_1^0$ | 162 | $\tilde{\tau}_1^\pm\tau^\mp$ | 99.6% | | |

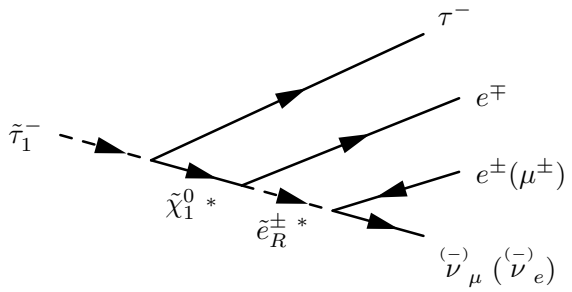


Figure 1: Illustration of the four body $\tilde{\tau}_1$ decay in the BC1 model.

The parameters are: the universal scalar ($m_0$) and gaugino ($m_{1/2}$) masses; the trilinear scalar coupling ($A_0$); the ratio of the Higgs vacuum expectation values ($\tan\beta$); the sign of the bilinear Higgs mixing parameter ($\mu$); and the coefficients from Equation (1) ($\mathbf{\Lambda}$), one of which is non-zero at the grand unification scale ($m_{\rm GUT}$).

The original BC1 benchmark point was proposed with the following parameters:

$$m_0 = A_0 = 0 \text{ GeV}; m_{1/2} = 400 \text{ GeV}; \tan\beta = 13; \mu > 0; \lambda_{121} = 0.032 \text{ at } m_{\rm GUT}. \quad (3)$$

The masses and decays of the lightest supersymmetric particles for this point are shown in Table 1, and the four body $\tilde{\tau}_1$ decay is illustrated in Figure 1. The model parameters are chosen to ensure a $\tilde{\tau}_1$ LSP. As pointed out in Ref. [9], the $\tilde{\tau}_1$ is a natural LSP in large regions of the mSUGRA/CMSSM parameter space, even for non-zero values of $m_0$ and $A_0$. The RPV coupling is small enough that SUSY particle pair production still dominates, but large enough that the $\tilde{\tau}_1$ LSP decays promptly. All sparticle cascades (except direct $\tilde{e}_R$ production) finish with the $\tilde{\tau}_1$ LSP, and may produce jets, soft $\tau$ leptons and other particles in the final state. The decay products of the two $\tilde{\tau}_1$ particles give some missing transverse momentum, two $\tau$ leptons, two electrons and a further two leptons in each event. This suggests that a search for anomalous events with multiple leptons would be very sensitive to this model. One such search strategy for this scenario was explored in Ref. [10]; here we use the results of the ATLAS four-lepton search.

In this note, we consider the $m_{1/2}$-$\tan\beta$ plane containing the original BC1 benchmark point. Across this plane, SOFTSUSY [11] is used to calculate the particle spectrum, while decay rates of all particles except the LSP are calculated with ISAWIG 1.200 and ISAJET 7.64 [12]. Theoretical and experimental constraints were taken into account when defining the relevant range of parameter values. Regions with tachyons or a non-$\tilde{\tau}_1$ LSP were not considered further, and experimental limits from LEP on the Higgs

mass (using HiggsBounds 3.6.1beta [13] and FeynHiggs 2.8.6 [14]) were also applied. Light $\tilde{\tau}_1$ leptons are not considered in this analysis, and a cutoff is applied at a $\tilde{\tau}_1$ mass of 80 GeV, motivated by direct searches at LEP for RPV and RPC $\tilde{\tau}_1$ decays [15].

We use a modified form of HERWIG [16] to generate the events and simulate the $\tilde{\tau}_1$ decays. Events are produced using an ATLAS parameter tune [17], MRST2007LO* parton density functions (PDFs) [18] and a fast detector simulation AtlFast-II. Differences between this and the full ATLAS detector simulation were found to be within statistical uncertainties. The simulated Monte Carlo (MC) events are reweighted according to the mean expected number of interactions per bunch crossing, to account for varying pileup conditions during data-taking. Cross sections for each SUSY production process are calculated to at least next-to-leading order (NLO) precision, using a procedure described in Section 5.

# 4 Analysis

The data analysis, described in Ref. [1], is based on data collected in 2011 corresponding to an integrated luminosity of 2.06 fb$^{-1}$. Key aspects of this analysis will be described again here.

Electrons are required to have a transverse energy ($E_{\mathrm{T}}$) of at least 10 GeV, and a pseudorapidity $|\eta|$ less than 2.47. In the barrel/endcap transition region, electrons must have $E_{\mathrm{T}} > 15$ GeV. The summed transverse momentum ($p_{\mathrm{T}}$) of tracks with $\Delta R = \sqrt{(\Delta\eta)^2 + (\Delta\phi)^2} < 0.2$ around the electron's track must be less than 10% of the electron $E_{\mathrm{T}}$.

Muons are required to have $p_{\mathrm{T}} > 10$ GeV and $|\eta| < 2.4$. In addition, the summed $p_{\mathrm{T}}$ of Inner Detector tracks within $\Delta R < 0.2$ of the muon track must be less than 1.8 GeV and the total calorimeter $E_{\mathrm{T}}$ within $\Delta R < 0.3$ of the muon must be less than 4 GeV.

Single lepton triggers are used in this analysis. To ensure a high and stable trigger efficiency, events without a triggered electron (muon) with an offline reconstructed $E_{\mathrm{T}} > 25$ GeV ($p_{\mathrm{T}} > 20$ GeV) are rejected. The trigger is not applied in simulated events; instead, they are weighted by the electron and muon trigger efficiencies measured in data.

Jets are reconstructed using the anti-$k_t$ algorithm [19] with a radius parameter of 0.4. Only jets with $E_{\mathrm{T}} > 20$ GeV and $|\eta| < 2.8$ are used. Jets within $\Delta R < 0.2$ of a reconstructed electron are discarded. If an electron or muon lies within $\Delta R < 0.4$ of any remaining jet, then the lepton is discarded. Following this, any electron-muon pair with $\Delta R < 0.1$ is discarded.

The missing transverse momentum ($E_{\mathrm{T}}^{\mathrm{miss}}$) is calculated using all reconstructed objects, including jets with $|\eta| < 4.9$, non-isolated muons and calorimeter deposits not associated with reconstructed objects.

Events are required to have a primary vertex with at least five associated tracks. Events where muons are reconstructed with a large longitudinal or transverse impact parameter are rejected as cosmic-ray candidates. A cut is applied on the invariant mass of lepton pairs ($\ell^+\ell^- = e^+e^-, \mu^+\mu^-$) of $m_{\ell^+\ell^-} > 20$ GeV to reject low mass contributions from Drell-Yan production, photon conversions and low mass dilepton resonances.

Two signal regions are defined: SR1 and SR2. In SR1, events are selected with at least four selected leptons and $E_{\mathrm{T}}^{\mathrm{miss}} > 50$ GeV. In SR2, a $Z$ boson veto of $|m_{\ell^+\ell^-} - m_Z| > 10$ GeV is additionally required for all $\ell^+\ell^-$ pairs.

# 5 Systematic uncertainties

The contributions from all Standard Model background processes are estimated using MC simulation, with specific data-driven cross-checks being performed for internal conversion, $t\bar{t}$ and $ZZ$ background contributions. Experimental systematics on the background estimation, described in Ref. [1], are dominated by MC statistical uncertainties, followed by the jet energy scale and resolution, and the electron

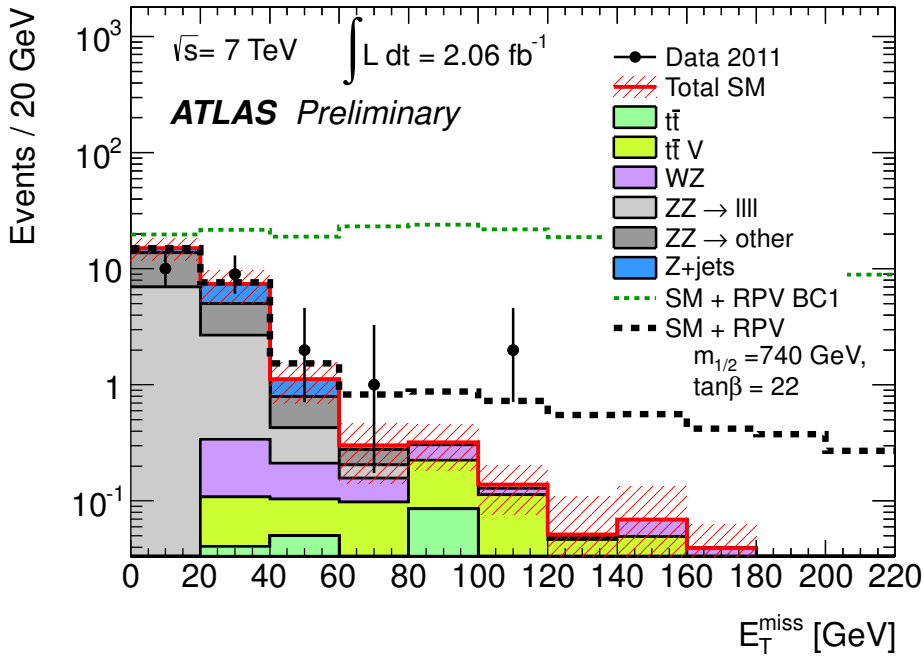


Figure 2: The $E_{\mathrm{T}}^{\mathrm{miss}}$ distribution for selected events before $E_{\mathrm{T}}^{\mathrm{miss}}$ and $Z$ veto cuts are applied. Both data and SM MC simulation are shown, together with the model predictions for the original BC1 benchmark point and another model point with $m_{1/2} = 740$ GeV and $\tan\beta = 22$. The hatched band represents systematic uncertainties on the SM background added in quadrature.

energy resolution. Experimental systematic uncertainties (energy scales, resolutions and detection efficiencies) are estimated for the signal model in the same way.

Signal cross sections are calculated to next-to-leading order in the strong coupling constant, including the resummation of soft gluon emission at next-to-leading-logarithmic accuracy (NLO+NLL) where possible [20, 21].[1] An envelope of cross section predictions is defined using the 68% CL ranges of the CTEQ6.6M [22] (including the $\alpha_S$ uncertainty) and MSTW2008NLO [23] PDF sets, together with independent variations of the factorisation and renormalisation scales by factors of two or one half. The nominal cross section value is taken to be the midpoint of the envelope and the uncertainty assigned is half the full width of the envelope, closely following the PDF4LHC recommendations [24].

In general, theoretical uncertainties are no larger than 20% anywhere in the parameter space considered. In certain regions, such as where $\tilde{\tau}_1$-$\tilde{\tau}_1$ pair production dominates at high $\tan\beta$, the uncertainty is much lower.

## 6 Results and interpretation

Figure 2 shows the expected SM background and the observed data from Ref. [1] before $E_{\mathrm{T}}^{\mathrm{miss}}$ or $Z$ veto requirements are applied, together with the BC1 benchmark point and another model point near the

[1] The NLL correction is used for squark and gluino production when the squark and gluino masses lie between 200 GeV and 2 TeV. Following the convention used in the NLO calculators the squark mass is defined as the average of the squark masses in the first two generations. In the case of gluino-pair (associated squark-gluino) production processes, the NLL calculations were extended up to squark masses of 4.5 TeV (3.5 TeV). For masses outside this range and for other types of production processes (i.e. electroweak and associated strong and electroweak) cross sections at NLO accuracy obtained with PROSPINO 2.1 [20] are used.

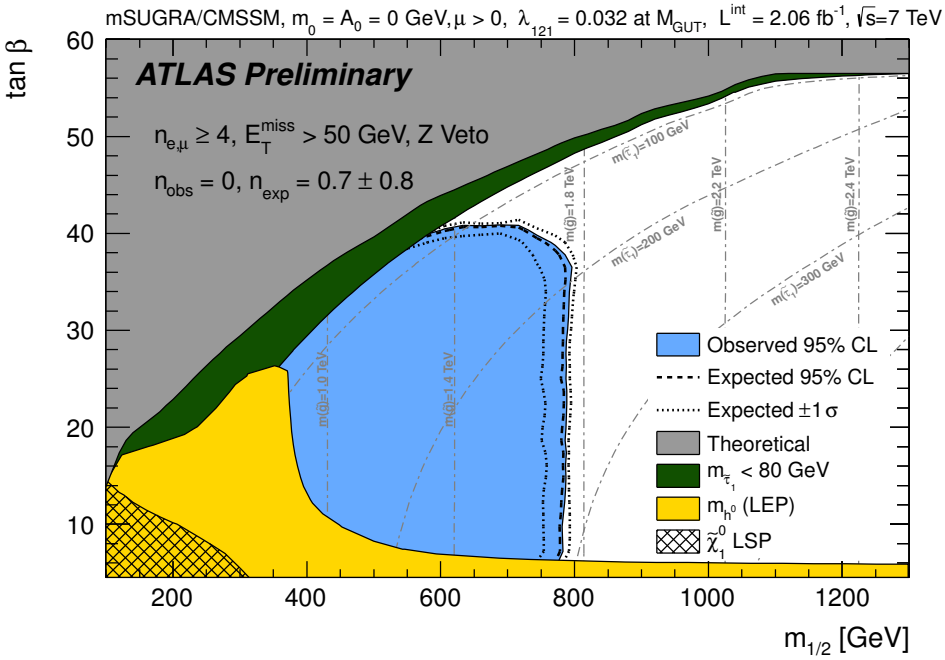


Figure 3: New excluded region (Observed) at 95% Confidence Level (CL) as a function of $m_{1/2}$ and $\tan\beta$ in signal region SR2. The expected exclusion and its $\pm 1\sigma$ variations are indicated by dashed lines. The other solid shaded areas are excluded from this analysis by LEP results on the Higgs mass [13] or because $m_{\tilde{\tau}_1} < 80$ GeV.

current sensitivity limit. No significant excess was found: in SR1, 4 events were observed, with $1.7 \pm 0.9$ expected from the Standard Model background; the equivalent numbers for SR2 were zero and $0.7 \pm 0.8$ events, respectively. SR2 is used to place limits on the BC1-like model, given its greater sensitivity to this scenario. Plots of the acceptance and efficiency of this selection can be found in Appendices A and B.

Limits were set using the profile likelihood procedure from Ref. [1], with the addition of the uncertainties on the signal model descibed in Section 5. Systematic uncertainties that affect both signal and background, such as the jet energy scale, are treated with appropriate correlations.

The observed and expected 95% Confidence Level (CL) exclusion limits are calculated with the $CL_s$ method and are shown in Figure 3. The region with $m_{1/2} < 800$ GeV is excluded, if $\tan\beta < 40$, corresponding to a limit on the gluino mass of approximately 1770 GeV within this range. As $\tan\beta$ increases, keeping $m_{1/2}$ fixed, reconstruction becomes more difficult due to changes in the $\tilde{\tau}_1$ lifetime and decay modes (see Figures 5 in Appendix A and 10 in Appendix B).

These results has been produced considering the single value $\lambda_{121}(m_{\rm GUT}) = 0.032$. Taking different values would affect the sparticle spectrum, but this effect is small below the upper limit of $\lambda_{121}(m_{\rm GUT}) = 0.1$ from neutrino mass constraints [4]. More significantly, lowering $\lambda_{121}$ would increase the $\tilde{\tau}_1$ lifetime, thus reducing the reconstruction efficiency. The current analysis is sensitive to $\tilde{\tau}_1$ LSPs with a lifetime $\lesssim O(1$ ps) (see Appendix B, especially Figure 10). Changing the value of $\lambda_{121}$ would therefore primarily affect the excluded region at high $\tan\beta$, where the $\tilde{\tau}_1$ lifetime is already within this range (Figure 5).

# 7 Conclusion

In this note, the results of a search for new physics in final states with four or more leptons and moderate missing transverse momentum are interpreted using an $R$-parity violating mSUGRA/CMSSM model

with $\lambda_{121} = 0.032$ at $m_{\text{GUT}}$ and $m_{\tilde{\tau}_1} > 80$ GeV. In 2.06 fb$^{-1}$ of data, no evidence for new physics was observed, and this model is excluded where $m_{1/2} < 800$ GeV and $\tan\beta < 40$ for $m_0 = A_0 = 0$ and $\mu > 0$.

## References


[1] ATLAS Collaboration, *Search for supersymmetry in events with four or more leptons and missing transverse momentum in pp collisions at $\sqrt{s} = 7$ TeV with the ATLAS detector*, ATLAS-CONF-2012-001.

[2] A. H. Chamseddine, R. L. Arnowitt, and P. Nath, *Locally Supersymmetric Grand Unification*, Phys. Rev. Lett. **49** (1982) 970.

R. Barbieri, S. Ferrara, and C. A. Savoy, *Gauge Models with Spontaneously Broken Local Supersymmetry*, Phys. Lett. **B119** (1982) 343.

L. E. Ibanez, *Locally Supersymmetric SU(5) Grand Unification*, Phys. Lett. **B118** (1982) 73.

L. J. Hall, J. D. Lykken, and S. Weinberg, *Supergravity as the Messenger of Supersymmetry Breaking*, Phys. Rev. **D27** (1983) 2359–2378.

N. Ohta, *Grand unified theories based on local supersymmetry*, Prog. Theor. Phys. **70** (1983) 542.

G. L. Kane, C. F. Kolda, L. Roszkowski, and J. D. Wells, *Study of constrained minimal supersymmetry*, Phys. Rev. **D49** (1994) 6173–6210, arXiv:hep-ph/9312272.

[3] R. Hempfling, *Neutrino Masses and Mixing Angles in SUSY-GUT Theories with explicit R-Parity Breaking*, Nucl. Phys. **B478** (1996) 3–30, arXiv:hep-ph/9511288.

M. A. Diaz, J. C. Romao, and J. W. F. Valle, *Minimal supergravity with R-parity breaking*, Nucl. Phys. **B524** (1998) 23–40, arXiv:hep-ph/9706315.

H. K. Dreiner, C. Luhn, and M. Thormeier, *What is the discrete gauge symmetry of the MSSM?*, Phys. Rev. **D73** (2006) 075007, arXiv:hep-ph/0512163.

H. K. Dreiner, C. Luhn, H. Murayama, and M. Thormeier, *Baryon Triality and Neutrino Masses from an Anomalous Flavor U(1)*, Nucl. Phys. **B774** (2007) 127–167, arXiv:hep-ph/0610026.

H.-S. Lee, *Minimal gauge origin of baryon triality and flavorful signatures at the LHC*, Phys. Lett. **B704** (2011) 316–321, arXiv:1007.1040 [hep-ph].

[4] B. Allanach, A. Dedes, and H. Dreiner, *R parity violating minimal supergravity model*, Phys. Rev. **D69** (2004) 115002, arXiv:hep-ph/0309196. Erratum ibid. D **72** (2005) 079902.

[5] H. Miyazawa, *Baryon Number Changing Currents*, Prog. Theor. Phys. **36 (6)** (1966) 1266–1276.

P. Ramond, *Dual Theory for Free Fermions*, Phys. Rev. **D3** (1971) 2415–2418.

Y. A. Golfand and E. P. Likhtman, *Extension of the Algebra of Poincare Group Generators and Violation of p Invariance*, JETP Lett. **13** (1971) 323–326. [Pisma Zh.Eksp.Teor.Fiz.13:452-455,1971].

A. Neveu and J. H. Schwarz, *Factorizable dual model of pions*, Nucl. Phys. **B31** (1971) 86–112.

A. Neveu and J. H. Schwarz, *Quark Model of Dual Pions*, Phys. Rev. **D4** (1971) 1109–1111.

J. Gervais and B. Sakita, *Field theory interpretation of supergauges in dual models*, Nucl. Phys. **B34** (1971) 632–639.

D. V. Volkov and V. P. Akulov, *Is the Neutrino a Goldstone Particle?*, Phys. Lett. **B46** (1973) 109–110.

J. Wess and B. Zumino, *A Lagrangian Model Invariant Under Supergauge Transformations*, Phys. Lett. **B49** (1974) 52.

J. Wess and B. Zumino, *Supergauge Transformations in Four-Dimensions*, Nucl. Phys. **B70** (1974) 39–50.

[6] S. Weinberg, *Supersymmetry at Ordinary Energies. 1. Masses and Conservation Laws*, Phys. Rev. **D26** (1982) 287.

N. Sakai and T. Yanagida, *Proton Decay in a Class of Supersymmetric Grand Unified Models*, Nucl. Phys. **B197** (1982) 533.

[7] P. Fayet, *Supersymmetry and Weak, Electromagnetic and Strong Interactions*, Phys. Lett. **B64** (1976) 159.

P. Fayet, *Spontaneously Broken Supersymmetric Theories of Weak, Electromagnetic and Strong Interactions*, Phys. Lett. **B69** (1977) 489.

G. R. Farrar and P. Fayet, *Phenomenology of the Production, Decay, and Detection of New Hadronic States Associated with Supersymmetry*, Phys. Lett. **B76** (1978) 575–579.

P. Fayet, *Relations Between the Masses of the Superpartners of Leptons and Quarks, the Goldstino Couplings and the Neutral Currents*, Phys. Lett. **B84** (1979) 416.

S. Dimopoulos and H. Georgi, *Softly Broken Supersymmetry and SU(5)*, Nucl. Phys. **B193** (1981) 150.

[8] H. Goldberg, *Constraint on the photino mass from cosmology*, Phys. Rev. Lett. **50** (1983) 1419.

J. Ellis, J. Hagelin, D. Nanopoulos, K. Olive, and M. Srednicki, *Supersymmetric relics from the big bang*, Nucl. Phys. **B238** (1984) 453–476.

[9] B. Allanach, M. Bernhardt, H. Dreiner, C. Kom, and P. Richardson, *Mass Spectrum in R-Parity Violating mSUGRA and Benchmark Points*, Phys. Rev. **D75** (2007) 035002, arXiv:hep-ph/0609263.

[10] K. Desch, S. Fleischmann, P. Wienemann, H. K. Dreiner, and S. Grab, *Stau as the Lightest Supersymmetric Particle in R-Parity Violating SUSY Models: Discovery Potential with Early LHC Data*, Phys. Rev. **D83** (2011) 015013, arXiv:1008.1580 [hep-ph].

[11] B. Allanach, *SOFTSUSY: a program for calculating supersymmetric spectra*, Comput. Phys. Commun. **143** (2002) 305–331, arXiv:hep-ph/0104145.

B. Allanach and M. Bernhardt, *Including R-parity violation in the numerical computation of the spectrum of the minimal supersymmetric standard model: SOFTSUSY3.0*, Comput. Phys. Commun. **181** (2010) 232–245, arXiv:0903.1805 [hep-ph].

[12] F. E. Paige, S. D. Protopopescu, H. Baer, and X. Tata, *ISAJET 7.69: A Monte Carlo event generator for pp, anti-p p, and e+e- reactions*, arXiv:hep-ph/0312045.

[13] P. Bechtle, O. Brein, S. Heinemeyer, G. Weiglein, and K. E. Williams, *HiggsBounds 2.0.0: Confronting Neutral and Charged Higgs Sector Predictions with Exclusion Bounds from LEP and the Tevatron*, Comput. Phys. Commun. **182** (2011) 2605–2631, arXiv:1102.1898 [hep-ph]. http://www.ippp.dur.ac.uk/HiggsBounds.

P. Bechtle, O. Brein, S. Heinemeyer, G. Weiglein, and K. E. Williams, *HiggsBounds: Confronting Arbitrary Higgs Sectors with Exclusion Bounds from LEP and the Tevatron*, Comput. Phys. Commun. **181** (2010) 138–167, arXiv:0811.4169 [hep-ph].

[14] M. Frank, T. Hahn, S. Heinemeyer, W. Hollik, H. Rzehak, et al., *The Higgs Boson Masses and Mixings of the Complex MSSM in the Feynman-Diagrammatic Approach*, JHEP **0702** (2007) 047, arXiv:hep-ph/0611326 [hep-ph].

G. Degrassi, S. Heinemeyer, W. Hollik, P. Slavich, and G. Weiglein, *Towards high precision predictions for the MSSM Higgs sector*, Eur. Phys. J. **C28** (2003) 133–143, arXiv:hep-ph/0212020 [hep-ph].

S. Heinemeyer, W. Hollik, and G. Weiglein, *The Masses of the neutral CP - even Higgs bosons in the MSSM: Accurate analysis at the two loop level*, Eur. Phys. J. **C9** (1999) 343–366, arXiv:hep-ph/9812472 [hep-ph].

S. Heinemeyer, W. Hollik, and G. Weiglein, *FeynHiggs: A Program for the calculation of the masses of the neutral CP even Higgs bosons in the MSSM*, Comput. Phys. Commun. **124** (2000) 76–89, arXiv:hep-ph/9812320 [hep-ph].

[15] Particle Data Group Collaboration, K. Nakamura et al., *Review of particle physics*, J. Phys. G **G37** (2010) 075021. 2011 and partial update for the 2012 edition.

[16] G. Corcella, I. Knowles, G. Marchesini, S. Moretti, K. Odagiri, et al., *HERWIG 6: An Event generator for hadron emission reactions with interfering gluons (including supersymmetric processes)*, JHEP **0101** (2001) 010, arXiv:hep-ph/0011363.

G. Corcella, I. Knowles, G. Marchesini, S. Moretti, K. Odagiri, et al., *HERWIG 6.5 release note*, arXiv:hep-ph/0210213.

S. Moretti, K. Odagiri, P. Richardson, M. H. Seymour, and B. R. Webber, *Implementation of supersymmetric processes in the HERWIG event generator*, JHEP **0204** (2002) 028, arXiv:hep-ph/0204123.

[17] *Charged particle multiplicities in p p interactions at $\sqrt{s}$ = 0.9 and 7 TeV in a diffractive limited phase-space measured with the ATLAS detector at the LHC and new PYTHIA6 tune*, Tech. Rep. ATLAS-CONF-2010-031, CERN, Geneva, Jul, 2010.

[18] A. Sherstnev and R. S. Thorne, *Parton Distributions for LO Generators*, Eur. Phys. J. **C55** (2008) 553–575, arXiv:0711.2473 [hep-ph].

[19] M. Cacciari, G. P. Salam, and G. Soyez, *The anti-$k_t$ jet clustering algorithm*, JHEP **04** (2008) 063, arXiv:0802.1189 [hep-ph].

M. Cacciari and G. P. Salam, *Dispelling the $N^3$ myth for the $k_t$ jet-finder*, Phys. Lett. **B641** (2006) 57–61, arXiv:hep-ph/0512210. http://fastjet.fr/.

[20] W. Beenakker, R. Hopker, M. Spira, and P. Zerwas, *Squark and gluino production at hadron colliders*, Nucl. Phys. **B492** (1997) 51–103, arXiv:hep-ph/9610490 [hep-ph].

[21] A. Kulesza and L. Motyka, *Threshold resummation for squark-antisquark and gluino-pair production at the LHC*, Phys. Rev. Lett. **102** (2009) 111802, arXiv:0807.2405 [hep-ph].

A. Kulesza and L. Motyka, *Soft gluon resummation for the production of gluino-gluino and squark-antisquark pairs at the LHC*, Phys. Rev. **D80** (2009) 095004, arXiv:0905.4749 [hep-ph].

W. Beenakker, S. Brensing, M. Kramer, A. Kulesza, E. Laenen, et al., *Soft-gluon resummation for squark and gluino hadroproduction*, JHEP **0912** (2009) 041, arXiv:0909.4418 [hep-ph].

W. Beenakker, S. Brensing, M. Kramer, A. Kulesza, E. Laenen, et al., *Squark and gluino hadroproduction*, Int. J. Mod. Phys. **A26** (2011) 2637–2664, arXiv:1105.1110 [hep-ph].

[22] P. M. Nadolsky et al., *Implications of CTEQ global analysis for collider observables*, Phys. Rev. **D78** (2008) 013004, arXiv:0802.0007 [hep-ph].

[23] A. Martin, W. Stirling, R. Thorne, and G. Watt, *Parton distributions for the LHC*, Eur. Phys. J. **C63** (2009) 189–285, arXiv:0901.0002 [hep-ph].

[24] M. Botje, J. Butterworth, A. Cooper-Sarkar, A. de Roeck, J. Feltesse, et al., *The PDF4LHC Working Group Interim Recommendations*, arXiv:1101.0538 [hep-ph].

# A Appendix: Model characteristics

In this Appendix, the characteristics of the BC1-like model are illustrated. Figure 4 shows the regions excluded from this analysis, while Figure 5 shows the lifetime and the four-body branching fraction of the $\tilde{\tau}_1$ LSP.

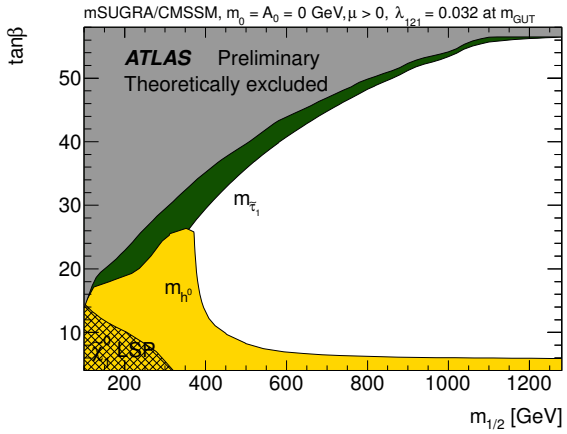


Figure 4: Characteristics of the $m_{1/2}$-tan$\beta$ plane in the BC1 scenario. The shaded regions include: a theoretically forbidden region producing tachyons, a region with a $\tilde{\chi}_1^0$ LSP, a region excluded by LEP Higgs bounds, and a region with $m_{\tilde{\tau}_1}$ below the 80 GeV threshold considered in this analysis.

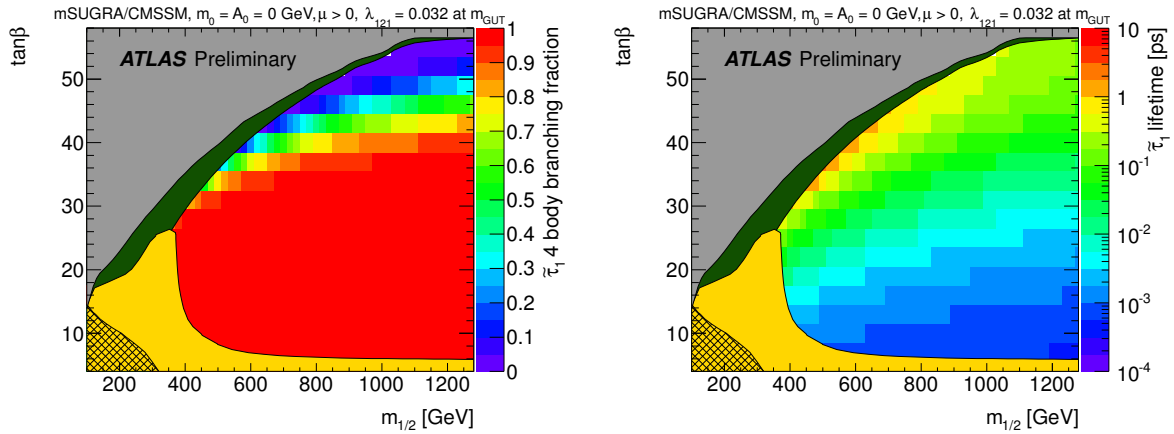


Figure 5: Branching ratio of the $\tilde{\tau}_1$ four-body decay (left) and the $\tilde{\tau}_1$ lifetime (right) as a function of $m_{1/2}$ and tan$\beta$. The solid shaded areas are excluded from this analysis, see Figure 4 for details.

# B Appendix: Analysis expectations

Some details of the expected analysis results are shown in this Appendix. Figure 6 shows the expected number of events in SR2 with this analysis. Figure 7 shows the total product of kinematic acceptance and selection efficiency, while Figure 8 shows the same for groups of SUSY production processes. The acceptance and efficiency are shown separately in Figures 9 and 10 respectively, while Figure 11 shows the expected fractional contribution to SR2 from each process group after the full event selection.

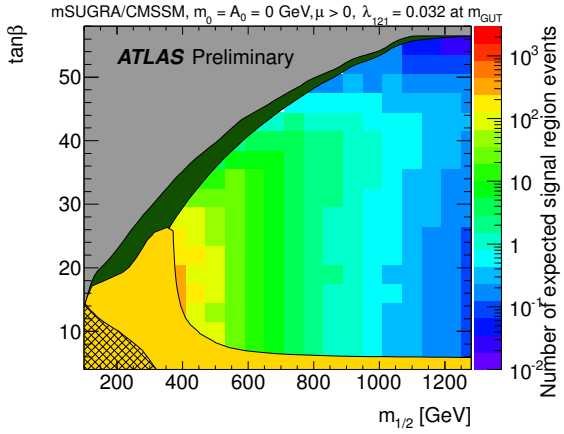


Figure 6: Number of signal events expected in SR2 for the BC1-like model points with 2.06 fb$^{-1}$ as a function of $m_{1/2}$ and $\tan\beta$. The solid shaded areas are excluded from this analysis, see Figure 4 for details.

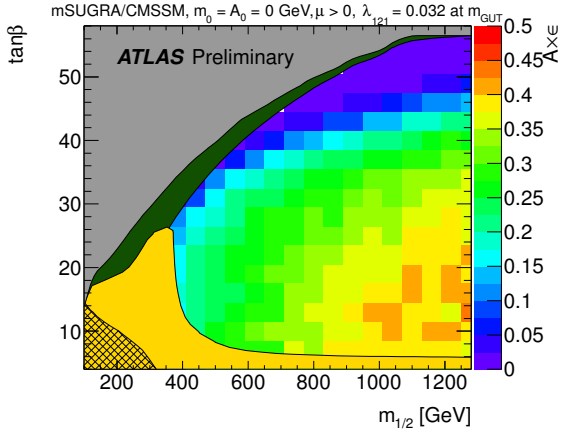


Figure 7: Signal acceptance times efficiency of the 4 lepton analysis for the BC1-like model points, averaged over all production processes as a function of $m_{1/2}$ and $\tan\beta$. The solid shaded areas are excluded from this analysis, see Figure 4 for details.

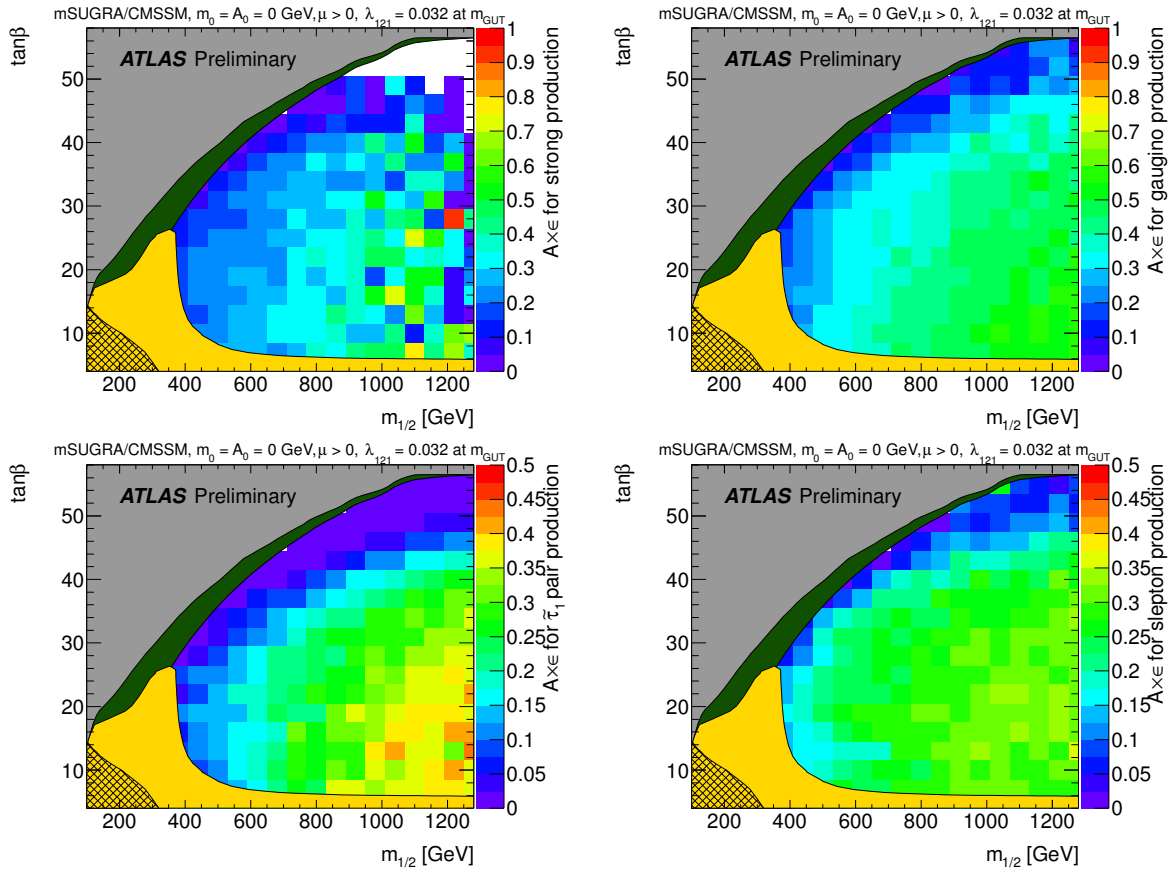


Figure 8: Signal acceptance times efficiency for strong production (top left), gaugino-gaugino (top right), $\tilde{\tau}_1$-$\tilde{\tau}_1$ (bottom left) and other $\tilde{\ell}$-$\tilde{\ell}$ (bottom right) production as a function of $m_{1/2}$ and $\tan\beta$. Statistical fluctuations can be seen, especially where the contributions to the signal region are small (see Figure 11). The solid shaded areas are excluded from this analysis, see Figure 4 for details.

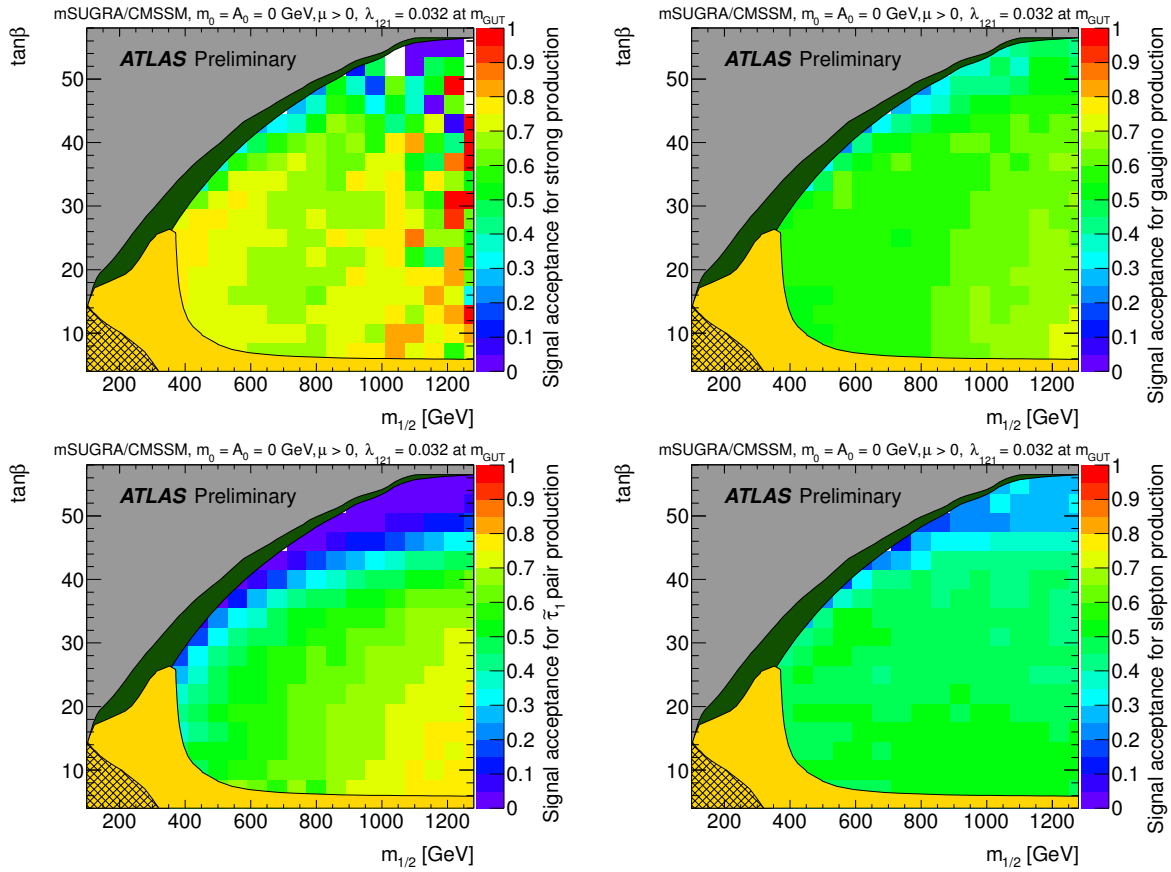


Figure 9: Signal acceptance for strong production (top left), gaugino-gaugino (top right), $\tilde{\tau}_1$-$\tilde{\tau}_1$ (bottom left) and other $\tilde{\ell}$-$\tilde{\ell}$ (bottom right) production as a function of $m_{1/2}$ and $\tan\beta$. Statistical fluctuations can be seen, especially where the contributions to the signal region are small (see Figure 11). The solid shaded areas are excluded from this analysis, see Figure 4 for details.

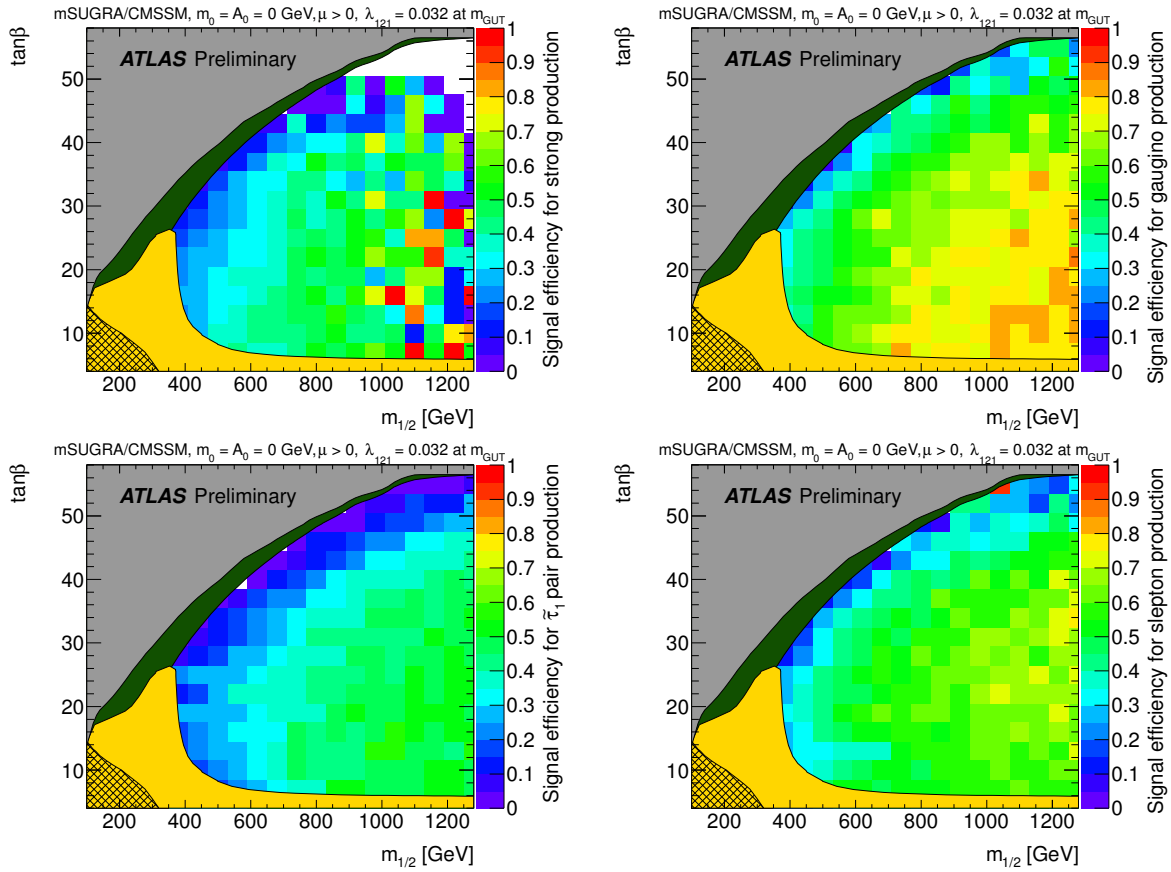


Figure 10: Signal efficiency for strong production (top left), gaugino-gaugino (top right), $\tilde{\tau}_1$-$\tilde{\tau}_1$ (bottom left) and other $\tilde{\ell}$-$\tilde{\ell}$ (bottom right) production as a function of $m_{1/2}$ and $\tan\beta$. Statistical fluctuations can be seen, especially where the contributions to the signal region are small (see Figure 11). The solid shaded areas are excluded from this analysis, see Figure 4 for details.

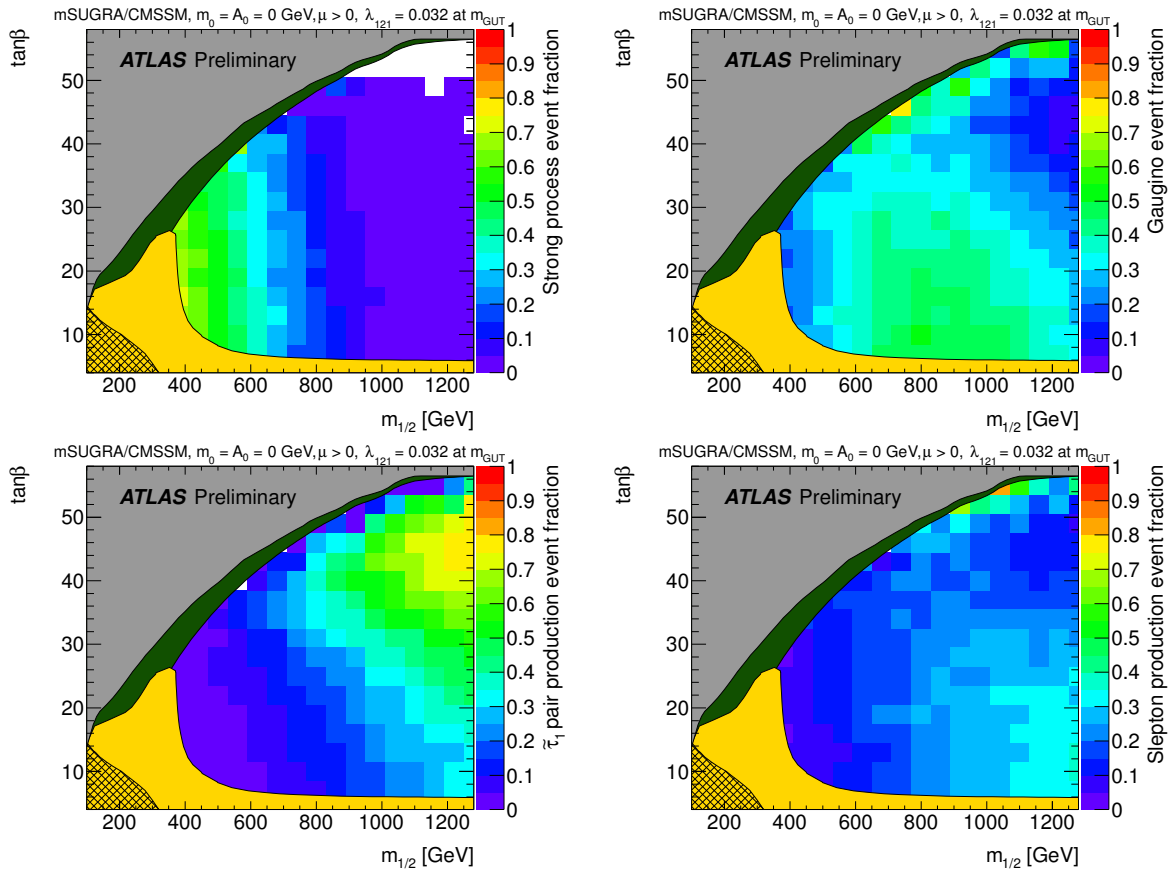


Figure 11: Relative contribution to the signal expectation from strong production (top left), gaugino-gaugino (top right), $\tilde{\tau}_1$-$\tilde{\tau}_1$ (bottom left) and other $\tilde{\ell}$-$\tilde{\ell}$ pairs (bottom right) production as a function of $m_{1/2}$ and $\tan\beta$. The solid shaded areas are excluded from this analysis, see Figure 4 for details.